GBT-BASED LOCAL AND GLOBAL BUCKLING ANALYSIS OF C-SECTION AND RHS STAINLESS STEEL COLUMNS

D. Camotim
Civil Engineering Department, IST, TU Lisbon, Portugal

R. Gonçalves
ESTB, Polytechnic Institute of Setúbal, Portugal

Abstract

A brief overview of the formulation of a non-linear elastic Generalised Beam Theory (GBT) is first presented. This formulation extends/modifies the available one and can be applied to assess the local and global buckling behaviour of open and closed thin-walled columns made of elastic-plastic materials, such as stainless steel or aluminium. Attention is focused on: (i) the specific modifications required to handle the material non-linearity and, as GBT includes genuine folded-plate theory concepts, (ii) the evaluation of the adequate instantaneous elastic moduli. Then, the GBT formulation is validated and used to investigate the buckling behaviour of C-section and RHS stainless steel columns. The material behaviour is modelled by means of a Ramberg-Osgood stress-strain law and both J_2 flow and deformation plasticity theories are employed.

1 INTRODUCTION

The use of stainless steel members for structural applications has grown rapidly in recent years, due to a combination of several factors, namely their: (i) structural efficiency, (ii) corrosion resistance and ease of maintenance, (iii) improved fire resistance, (iv) pleasing appearance and, last but not least, (v) increasingly competitive prices [1,2]. On the other hand, cost efficiency and aesthetic demands often lead to the choice of rather slender thin-walled members, which are highly susceptible to local-plate, distortional and/or global buckling phenomena. In fact, it is well known that (i) the strength (load-carrying capacity) of such members is mostly governed by the above buckling phenomena and that (ii) economic designs may only be achieved if the methods used to determine their structural behaviour include an accurate material modelling [1,3]. In this respect, note that the current Eurocode (ENV document) for stainless steel structures [4] “borrows“ the carbon steel elastic-perfect plastic material model, which means that it (i) neglects all the beneficial effects stemming from taking into account strain-hardening and, therefore, (ii) leads to overly conservative (uneconomic) designs [1,3].

Unlike carbon steel, stainless steel exhibits a non-linear stress-strain law, often including a considerable amount of strain-hardening [1,2]. This behavioural difference implies that buckling (bifurcation) phenomena, either local or global, often occur in the non-linear (elastic-plastic) range, thus meaning that it is necessary to assess the evolution of the elastic moduli along the member fundamental equilibrium path, a procedure requiring load incrementation during the pre-buckling stage. In this respect, it is worth recalling that the plastic bifurcation of elastic-plastic solids, (i) is fully governed by the active (instantaneous) elastic moduli and, (ii) in columns (uniformly compressed members), always takes place under increasing load [5,6]). Therefore, the bifurcation load of an elastic-plastic column can be determined by performing the stability analysis of its “hypoelastic counterpart” (*e.g.*, [7,8]).

In order to accurately assess both the local (plate) and global (member) buckling behaviour of stainless steel thin-walled columns, one must be able to model adequately (i) the cross-section deformations and (ii) the material 3-D incremental non-linear constitutive relation, a task which requires knowing: (a) an initial yield surface (elastic/proportionality limit), (b) a strain-hardening rule (yield surface evolution) and (c) a flow rule (incremental plastic strain vector direction). Thus, practically all geometrically non-linear analyses of such columns must be performed by means of finite element (FE) or finite strip (FS) analyses, adopting refined meshes and employing computationally intensive numerical techniques [9]. In this respect, it is still worth mentioning the “plate buckling paradox”, which is (i) related to fact that compressed plated structures develop two-dimensional stress states during buckling [9] and (ii) described by Hutchinson [7] as follows: “It was discovered that bifurcation loads calculated using the simplest flow theories of plasticity consistently overestimated buckling loads of plates and shells obtained in tests.

Calculations based on the less respectable deformation theories of plasticity gave reasonably good agreement with test results".

Generalised Beam Theory (GBT) was originally developed by Schardt [10], about two decades ago and in the context of linear elastic isotropic materials, and subsequently employed by Davies *et al* [11,12] to investigate the buckling behaviour of cold-formed steel profiles. Quite recently, Silvestre & Camotim [13,14]) have extended GBT to (linear elastic) orthotropic materials, thus enabling its use to study the buckling behaviour of composite or laminated plate thin-walled members. In both cases, GBT has been shown to be a rather powerful and clarifying analytical tool to assess the local and global buckling behaviour of thin-walled prismatic members. Indeed, it seems fair to say that it has been established as a valid and often advantageous alternative to fully numerical FE or FS analyses, mostly because it (i) incorporates genuine folded-plate theory (recall that it is a "beam theory") and (ii) has unique modal decomposition features.

The aim of this paper is to present a brief overview of the formulation of a non-linear elastic GBT, recently developed by the authors [15,16], which extends/modifies the available one in order to enable its application to investigate the buckling behaviour of open and closed thin-walled columns made of non--linear elastic-plastic materials, such as stainless steel or aluminium. Next, since GBT includes genuine folded-plate theory concepts, some attention must be devoted to the evaluation of the adequate instantaneous elastic moduli, an issue involving the choice of a given set of flow and strain-hardening rules and which has implications on the GBT procedure. Finally, several numerical results are presented and discussed, in order to validate and illustrate the application and capabilities of the proposed non-linear GBT. Such results concern (i) uniformly compressed rectangular plates (mostly for validation and accuracy studies) and (ii) C-section and rectangular hollow section (RHS) stainless steel columns. In all cases, (i) the material (stainless steel) uniaxial stress-strain law is modelled using the Ramberg-Osgood expression [17,18] and, because of the "plate buckling paradox" addressed earlier, (ii) both J_2 flow and deformation small strain plasticity theories are employed [19].

2 GBT EQUATION FOR NON-LINEAR MATERIALS

2.1 GBT fundamental equation

Before addressing the extension of the available (linear elastic) GBT to non-linear elastic materials, it is convenient to mention that the standard GBT procedure to perform buckling (linear stability) analyses comprises two main tasks, which can be briefly described as follows [10,13,14]:

(i) *Cross-section Analysis*. The member cross-section is subdivided into a set of straight wall (plate) elements, separated by natural and intermediate nodes. The warping (u) and transverse (w) displacements (see Figure 1) at the natural and intermediate nodes, respectively, constitute the *initial* cross-section degrees-of-freedom. In order to obtain the complete cross-section deformed configuration corresponding to each degree-of-freedom, unit displacements are sequentially imposed to the cross-section, which is then analysed as a deformable folded-plate. After completing this procedure, one is led to a set of fully populated stiffness and geometrical matrices, the components of which have no obvious physical meaning. Then, by means of a special coordinate transformation, which is a key step in the application of GBT, one: (a) diagonalises two stiffness matrices, (b) identifies the cross-section deformation modes (their amplitudes are the *final* degrees-of-freedom) and (c) evaluates the associated modal mechanical and geometrical properties.

(ii) *Member Analysis*. After performing the cross-section analysis, one is led to a system of differential equilibrium equations (one per deformation mode) and boundary conditions, involving the member: (a) cross-section modal mechanical and geometrical properties, (b) length value, (c) end support conditions and (d) applied loads. This system of equations defines a standard eigenvalue problem, which must then be solved, either analytically or numerically, to yield the bifurcation load parameter values (eigenvalues) and the corresponding buckling mode shapes (eigenvectors), expressed as linear combinations of the GBT deformation modes (*i.e.*, of functions describing their variation along the member longitudinal axis).

Since the application of GBT to perform bifurcation analyses in thin-walled members with *closed* (unicellular) cross-sections is still rather scarce, it deserves a few words. With respect to the "conventional" GBT analysis (open-section thin-walled members), the major difference consists of the need to incorporate an additional cross-section deformation mode, which accounts for Bredt's torsion. As shown by Schardt [10], this mode corresponds to the cross-section deformation due to a uniform shear

flow acting along its (closed) mid-line and is obtained by ignoring Vlassov's assumption of null membrane (plate) shear strains (still used to obtain all the other deformation modes). Therefore, it is characterised by (i) membrane (plate) shear distortion and, in the general case, also by (ii) transverse plate bending.

When dealing with non-linear elastic (hypoelastic) materials, both the cross-section and member analyses have to be modified, mostly due to the need to account for the evolution of the instantaneous elastic moduli along the fundamental path. This implies that it is indispensable to perform a numerical (incremental) pre-buckling analysis of the member, which (i) must include the adopted material properties and (ii) provides the characterisation (stress and instantaneous elastic moduli values) of the fundamental equilibrium states associated to each applied load level. Then, at any given fundamental state, assumed to be completely characterised, the bifurcation analysis consists of investigating whether there exists, for the hypoelastic (incrementally linear elastic) column, an adjacent state satisfying equilibrium. In other words, one searches for an incremental equilibrium state in the immediate vicinity of the fundamental (stressed) state, a procedure that requires using the rate form of the principle of virtual work, expressed by $\delta\dot{W} = \delta\dot{W}_e + \delta\dot{W}_i = 0$, where $\delta\dot{W}_e$ and $\delta\dot{W}_i$ are the rates of the external and internal virtual work.

Consider a column with an arbitrary thin-walled (open or closed) cross-section, where u, v and w are the mid-plane displacements, along the (local) x, y and z directions, of its wall elements (see Figure 1). In any given fundamental state, the column is subjected to uniform applied axial normal stresses $\sigma_{xx}=-P/\Omega$, where P is the applied compressive load, Ω is the cross-sectional area and the associated instantaneous elastic moduli values are deemed known (from the pre-buckling analysis). Then, the external and internal virtual work rates, at this fundamental state, read

$$\delta\dot{W}_e = \int_V \sigma_{xx}\,\delta\dot{u}_{,x}\,\mathrm{d}V = -\int_V \frac{P}{\Omega}\,\delta\dot{u}_{,x}\,dV \qquad \delta\dot{W}_i = -\int_V (\sigma_{ij}+\dot{\sigma}_{ij})\delta\dot{\varepsilon}_{ij}\,\mathrm{d}V = -\int_V \left(-\frac{P}{\Omega}\delta\dot{\varepsilon}^{M}_{xx}+\dot{\sigma}_{ij}\,\delta\dot{\varepsilon}_{ij}\right)dV \tag{1}$$

where (i) σ_{ij} are the stress tensor components at the fundamental state ($\sigma_{xx}=-P/\Omega$ is the only non null one), (ii) $\dot{\sigma}_{ij}$ is the stress-rate tensor, related to the strain-rate tensor $\dot{\varepsilon}_{ij}$ through the instantaneous elastic moduli ("hypoelastic column"), (iii) $\delta\dot{\varepsilon}_{ij}$ is the strain-rate tensor variation and (iv) the membrane longitudinal strain-rate variation is given by:

$$\delta\dot{\varepsilon}^{M}_{xx} = \delta\dot{u}_{,x} + \delta(\dot{v}^2_{,x} + \dot{w}^2_{,x})/2 \tag{2}$$

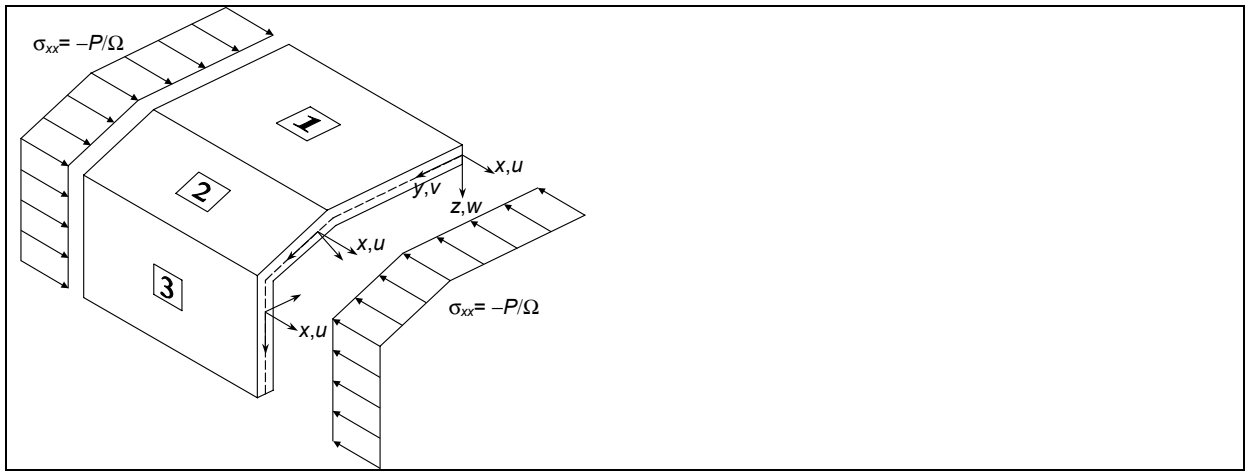

Figure 1 Thin-walled column geometry and local (wall element) axes

Finally, after incorporating equations (1) and (2) into the rate form of principle of virtual work, it becomes

$$\delta\dot{W} = -\int_V \frac{P}{\Omega}\,\delta\dot{u}_{,x}\,\mathrm{d}V - \int_V \left(-\frac{P}{\Omega}\,\delta\dot{\varepsilon}^{M}_{xx} + \dot{\sigma}_{ij}\,\delta\dot{\varepsilon}_{ij}\right)\mathrm{d}V = \int_V \left(\frac{P}{\Omega}\frac{\delta(\dot{v}^2_{,x}+\dot{w}^2_{,x})}{2} - \dot{\sigma}_{ij}\,\delta\dot{\varepsilon}_{ij}\right)\mathrm{d}V = 0 \tag{3}$$

and provides the means to ensure the hypoelastic column adjacent equilibrium. Then, (i) following the standard GBT procedure [13,14] and (ii) noticing that *rate* quantities are now involved, one is led to the GBT fundamental equation system

$$\boldsymbol{C}\{\dot{\phi}_{,xxxx}\} - \boldsymbol{D}\{\dot{\phi}_{,xx}\} + \boldsymbol{B}\{\dot{\phi}\} + P\,\boldsymbol{X}_1\{\dot{\phi}_{,xx}\} = \{0\} \tag{4}$$

where $\boldsymbol{C}$, $\boldsymbol{D}$, $\boldsymbol{B}$ and $\boldsymbol{X}_1$ are the usual GBT matrices ($\boldsymbol{X}_1$ is the geometric stiffness matrix related to uniform compression), evaluated on the basis of the instantaneous elastic moduli, and the components of vector $\{\dot{\phi}\}$ are functions providing the mode amplitude rates (which combine to yield the buckling modes).

2.2 Constitutive relations

In the case of an hypoelastic plate acted only by longitudinal stresses σ_{xx} (in the fundamental path), the incremental stress-strain relations read

$$\begin{Bmatrix} \dot{\sigma}_{xx}^{B} \\ \dot{\sigma}_{yy}^{B} \\ \dot{\sigma}_{xy}^{B} \end{Bmatrix} = \begin{bmatrix} \dot{E}_{11} & \dot{E}_{12} & 0 \\ \dot{E}_{21} & \dot{E}_{22} & 0 \\ 0 & 0 & \dot{E}_{33} \end{bmatrix} \begin{Bmatrix} \dot{\varepsilon}_{xx}^{B} \\ \dot{\varepsilon}_{yy}^{B} \\ \dot{\varepsilon}_{xy}^{B} \end{Bmatrix}, \quad \dot{\sigma}_{xx}^{M} = E_T \dot{\varepsilon}_{xx}^{M} \tag{5}$$

where $\dot{E}_{ij}$ are the instantaneous elastic moduli, E_T is the uniaxial (longitudinal) tangent modulus and the superscripts (^{B}) and (^{M}) identify the bending and membrane stress and strain-rates.

In this paper, the 3-D stainless steel material behaviour is described using the rate (incremental) form of the isotropic small strain J_2 (von Mises) flow and deformation theories of plasticity [19]. According to J_2 (i) flow [20] and (ii) deformation [21] theories of plasticity, the instantaneous elastic moduli associated with initial uniaxial stress states (note that column bifurcation always falls into this category) read, respectively,

$$\dot{E}_{11} = \frac{(\Lambda_T+3)E_0}{(5-4\nu)\Lambda_T-(1-2\nu)^2}, \quad \dot{E}_{22} = \frac{4\Lambda_T E_0}{(5-4\nu)\Lambda_T-(1-2\nu)^2}, \quad \dot{E}_{12} = \dot{E}_{21} = \frac{(4\nu+2\Lambda_T-2)E_0}{(5-4\nu)\Lambda_T-(1-2\nu)^2}, \quad \dot{E}_{33} = 2G \tag{6}$$

and

$$\dot{E}_{11} = \frac{(\Lambda_T+3\Lambda_S)E_0}{(2+3\Lambda_S-4\nu)\Lambda_T-(1-2\nu)^2}, \qquad \dot{E}_{22} = \frac{4\Lambda_T E_0}{(2+3\Lambda_S-4\nu)\Lambda_T-(1-2\nu)^2}$$

$$\dot{E}_{12} = \dot{E}_{21} = \frac{(4\nu+2\Lambda_T-2)E_0}{(2+3\Lambda_S-4\nu)\Lambda_T-(1-2\nu)^2}, \quad \dot{E}_{33} = \frac{2E_0}{2\nu-1+3\Lambda_S} \tag{7}$$

where E_0 is the initial (uniaxial) elastic modulus, ν is Poisson's ratio, G is the shear modulus, $\Lambda_T=E_0/E_T$ and $\Lambda_S=E_0/E_S$ (E_S being the uniaxial secant modulus).

Obviously, both the Λ_T and Λ_S values depend on the applied load (stress) level and are obtained from a suitable uniaxial stress-strain law (curve) describing the material behaviour along the fundamental path. In stainless steel structural applications, the well-known Ramberg-Osgood expression [17, 18]

$$\varepsilon = \frac{\sigma}{E_0} + 0.002\left(\frac{\sigma}{\sigma_{0.2}}\right)^n \tag{8}$$

where $\sigma_{0.2}$ is the 0.2% proof stress and the n is the strain-hardening parameter, is often employed and, therefore, it is also adopted in this work. Notice, however, that recent work by Mirambell & Real [22] has shown that the stainless steel uniaxial stress-strain law is best approximated by two adjoining Ramberg-Osgood curves, which are valid, respectively, (i) up to and (ii) beyond the proof stress $\sigma_{0.2}$ [1]. This more accurate stress-strain law can be easily incorporated in the formulated non-linear GBT, a task which (i) was not yet performed due to lack of time and (ii) is planned for the near future.

The incorporation of the above rate constitutive relations makes it necessary to modify the standard GBT procedure. Indeed, since the column "wall element" (plate) transverse displacements w are determined by means of the force method (*e.g.*, [10, 14]), the corresponding transverse bending stiffness

$$K_{22} = \frac{t^3}{12}\dot{E}_{22} \tag{9}$$

where t is the wall thickness, must be evaluated using an instantaneous transverse moduli $\dot{E}_{22}$ determined by means of (6) or (7). Obviously, if $\Lambda_T=\Lambda_S=1$ (linear elastic material), one obtains, in either case, the well-known elastic plate bending stiffness $K_{22,el}=t^3E_0/12(1-\nu^2)$.

It is a well-known fact that flow and deformation theories exhibit major differences regarding the evolution of the instantaneous elastic moduli along a uniaxial normal stress loading path [7] – indeed, the evolution of the instantaneous shear modulus $\dot{G}=\dot{E}_{33}/2$ provides a classic example of these differences: while for

flow theory one has always $\dot{G}=G$, for deformation theory $\dot{G}$ tends to zero as Λ_S increases. Since the plate transverse bending stiffness K_{22} plays a key role in the GBT procedure, it is worth examining how the ratio $\eta=K_{22}/K_{22,el}$ evolves according to both theories:

(i) According to flow theory, η depends only on Λ_T and ν. For instance, if $\nu=0.3$ one has $0.96<\eta\leq 1$ and it is possible to conclude that adopting the elastic stiffness $K_{22,el}$ (instead of K_{22}) leads to small errors, regardless of the Λ_T value.

(ii) According to deformation theory, on the other hand, η depends on Λ_T, Λ_S and ν (note, however, that Λ_T and Λ_S are not independent) and extremely small η values can be reached. Note that this is in sharp contrast with the behaviour according to flow theory.

The curves depicted in Figure 2 provide a clear illustration of the difference between the η values obtained according to both theories, for the particular case of E_0=200GPa, $\sigma_{0.2}$=300MPa, ν=0.3 and n=5.

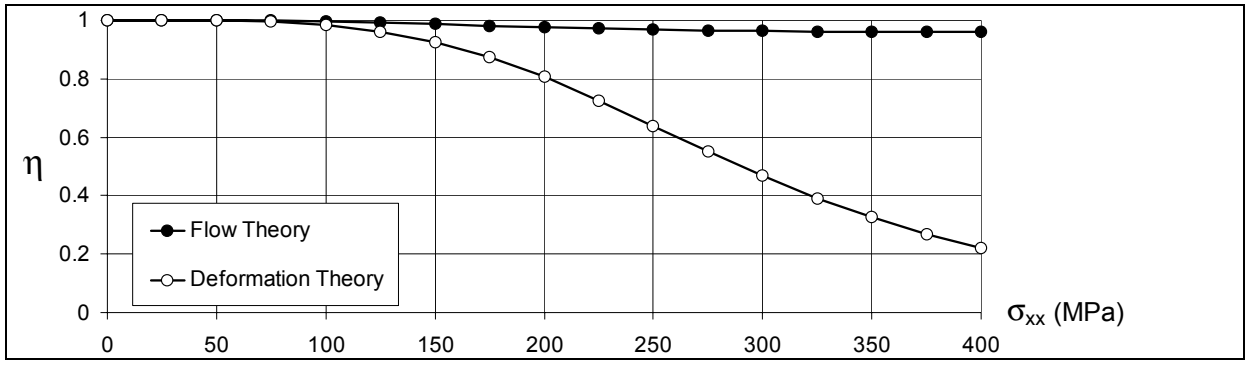

Figure 2 Evolution of the transverse bending stiffness ratio η with the longitudinal stress level

3 VALIDATION AND ILLUSTRATIVE EXAMPLES

3.1 Validation example: uniformly compressed rectangular plates

The buckling behaviour of uniformly compressed simply supported elastic-plastic rectangular plates (see Figure 3) was investigated by Handelman & Prager [20], who derived the analytical solution

$$\sigma_{cr} = \frac{\pi^2 m^2}{ta^2}\left[K_{22}\left(\frac{a^2}{m^2b^2}+\frac{K_{12}}{K_{22}}\right)^2 + K_{11} - \frac{K_{12}^2}{K_{22}}\right] \tag{10}$$

$$K_{11} = \frac{t^3}{12}\dot{E}_{11}, \quad K_{22} = \frac{t^3}{12}\dot{E}_{22}, \quad K_{12} = \frac{t^3}{12}\left[\dot{E}_{12}+\dot{E}_{33}\right] \tag{11}$$

where t is the plate thickness, a and b are the plate length and width and m is the number of longitudinal half-waves exhibited by the buckling mode.

In order to validate and assess the accuracy of the results provided by the developed GBT formulation, they are next compared with their "exact" counterparts, yielded by (10). The particular set of numerical results displayed concerns a plate with the following geometrical and material characteristics: t=2mm, b=100mm, E_0=200GPa, $\sigma_{0.2}$=300MPa, ν=0.3 and n=5 (Ramberg-Osgood). Only three equally-spaced intermediate nodes were considered in the GBT analysis and the corresponding deformation modes, depicted in Figure 3, exhibit only transverse displacements w, which satisfy the end conditions $w(0)=w(b)=0$ (the plate is simply supported along the four edges). Moreover, note that, in this case, (i) the GBT equation system is *uncoupled* and (ii) the plate critical buckling mode always coincides with GBT deformation mode 1.

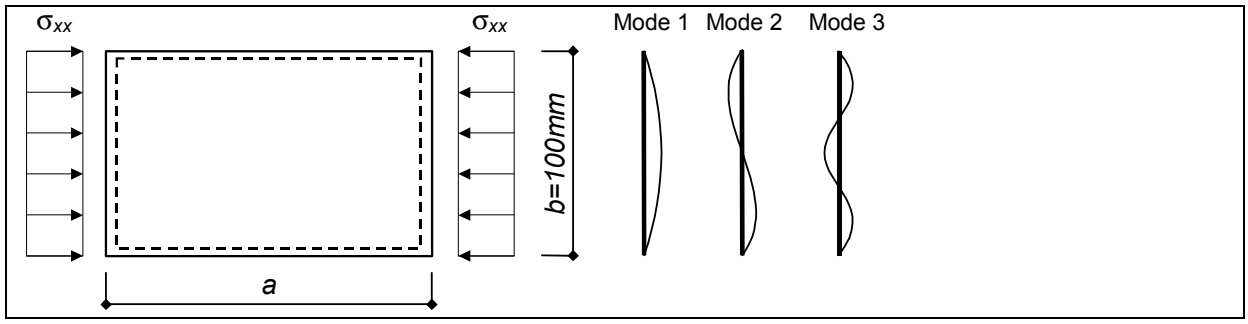

Figure 3 Rectangular plate geometry and GBT deformation modes

Figure 4 displays analytical and GBT-based critical buckling stresses σ_{cr} associated to three different material behaviours: (i) linear elastic (making $\Lambda_T=\Lambda_S=1$ in (10)), (ii) elastic-plastic behaviour with J_2 flow theory and (iii) elastic-plastic behaviour with J_2 deformation theory.

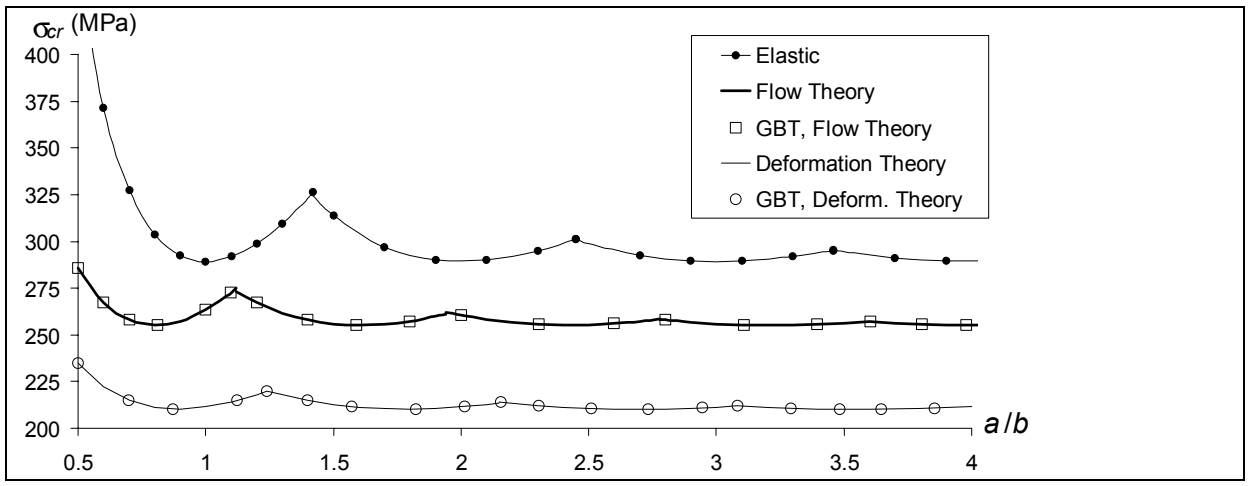

Figure 4 Critical buckling stress values for the rectangular plate

The observation of these results leads to the following remarks:

(i) Since the elastic-plastic plates bifurcate in the non-linear range, their critical stresses differ significantly from the linear elastic values. Obviously, the differences are higher for very short plates ($a/b<1$).

(ii) The results confirm that deformation theory leads to lower critical load values than flow theory [8].

(iii) GBT provides virtually exact results, even if only 3 intermediate nodes have been considered. The computational effort involved is much smaller than the one required by similar FE or FS analyses.

3.2 Illustrative example: C-section columns

Consider now the buckling behaviour of simply supported C-section columns with free-to-warp end sections and the cross-section dimensions indicated in Figure 5. The material properties are as in the previous example (E_0=200GPa, ν=0.3, $\sigma_{0.2}$=300MPa, n=5) and the cross-section is discretised using 6 natural nodes and 7 auxiliary ones (3 web intermediate nodes, 1 intermediate node per flange and 1 end node in each lip). This means that 13 deformation modes are involved: (i) the 4 classical rigid-body modes (extension, major and minor axis bending and torsion), (ii) 2 distortional modes and (iii) 7 local-plate modes. The shapes of the first (most relevant) 8 modes are depicted in Figure 5 and it should also be mentioned that all the analyses performed included only 11 modes. Indeed, the remaining two modes play absolutely no role and their suppression led to some computational savings, while retaining the same (very high) level of accuracy.

The curves presented in Figures 6(a)–(c) show the variation of the critical (bifurcation) stress σ_{cr}, associated to single half-wave buckling modes (m=1), with the column length L, for $L \geq 3$ cm (it makes no sense to analyse shorter columns). They correspond to the three material behaviours considered previously: (i) linear elastic, (ii) elastic-plastic with J_2 flow theory and (iii) elastic-plastic with J_2 deformation

theory. In each case, the curves concern buckling (i) in individual deformation modes (thin lines) and (ii) accounting for all deformation modes (thick line). Moreover, the participation factors of the GBT deformation modes in the column buckling mode are plotted in the diagrams shown in the bottom of Figures 6(a)–(c), which (i) stem from the unique GBT mode decomposition feature, (ii) provide insight on the nature of the different buckling mode shapes and (iii) help in visualising them.

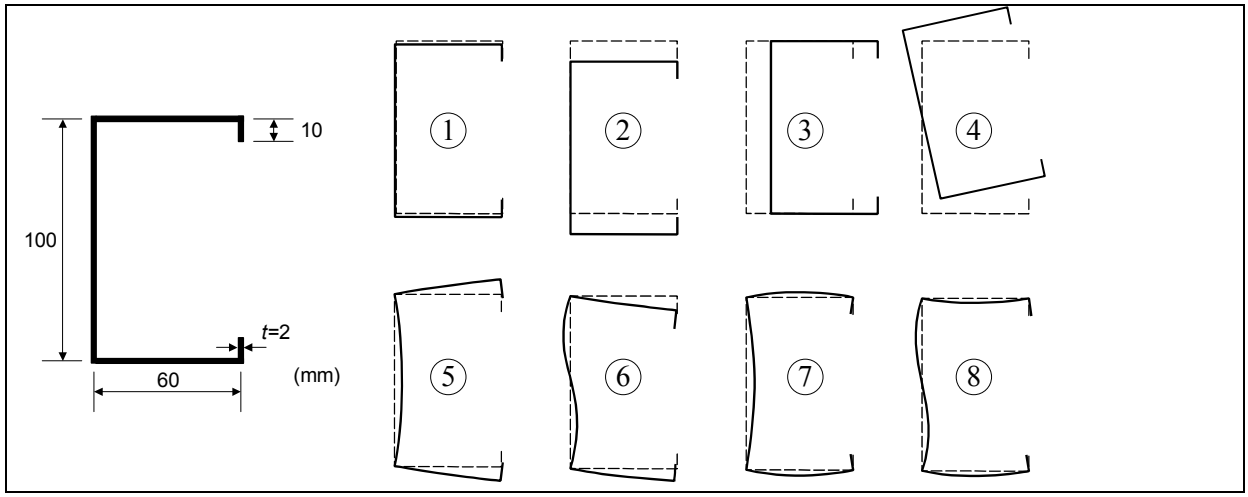

Figure 5 C-section column cross-section geometry and first eight GBT deformation mode shapes

After observing the set of results shown in Figures 6(a)–(c), the following conclusions can be drawn:

(i) The linear elastic curves (Figure 6(a)) fully agree with the results obtained for lipped channel cold-formed carbon steel columns and reported by Silvestre *et al* [23]. In particular, one confirms that, concerning the mode participation: (a) very short columns buckle in the web-triggered local plate mode ⑦, (b) the symmetric distortional mode ⑤ prevails for short columns, (c) mixed distortional-flexural-torsional modes (②+④+⑥) appear for intermediate columns, (d) flexural-torsional modes (②+④) occur for long columns and (e) very long columns buckle in a weak-axis flexural mode ③.

(ii) Obviously, the elastic-plastic bifurcation stresses are lower than the elastic ones, except for very long columns, which buckle when $\Lambda_T \approx \Lambda_S \approx 1$. As for the plate, deformation theory leads to lower *local* critical loads than flow theory. Moreover, the elastic-plastic curves exhibit smoother transitions between local-plate and distortional or distortional and global critical buckling modes.

(iii) The flow theory individual distortional curves (Figure 6(b)) somehow "combine" the descending (left) branches obtained using deformation theory (small slopes) with the linear elastic ascending ones (high slopes). This is due to the fact that (a) while the former are mostly governed by the tangent modulus E_T (identical for the flow and deformation theories), (b) the latter are mainly influenced by the value of K_{22} (very similar for the flow theory and linear elastic material models).

(iv) The curves concerning the individual flexural modes (②, ③) virtually reproduce the values yielded by analytical tangent modulus formulae. Moreover, the curves associated to the torsional (④) and symmetric distortional (⑤) modes also agree with analytical results recently obtained by the authors and which will be reported in the near future.

Figure 6(d) shows plots of "all mode" curves associated to (i) single half-wave buckling (m=1 – thin lines) and (ii) "true" critical stresses, obtained by considering buckling modes with several half-waves ($m \geq 1$ – thick lines), which concern the material behaviours dealt with in this work. After comparing the three pairs of curves, one concludes that:

(i) The "true" linear elastic curve coincides again with the one determined for lipped channel cold-formed carbon steel columns [23]. Critical buckling modes with $m>1$ occur only for column lengths associated to transitions between (a) local-plate and distortional or (b) distortional and flexural-torsional modes.

(ii) In the column length range associated to the transition between local-plate and distortional critical buckling modes, the "true" elastic-plastic (flow and deformation) curves correspond, virtually always (there is a very minor exception), to single half-wave buckling modes (m=1). Note that is clearly not the case for the linear elastic columns.

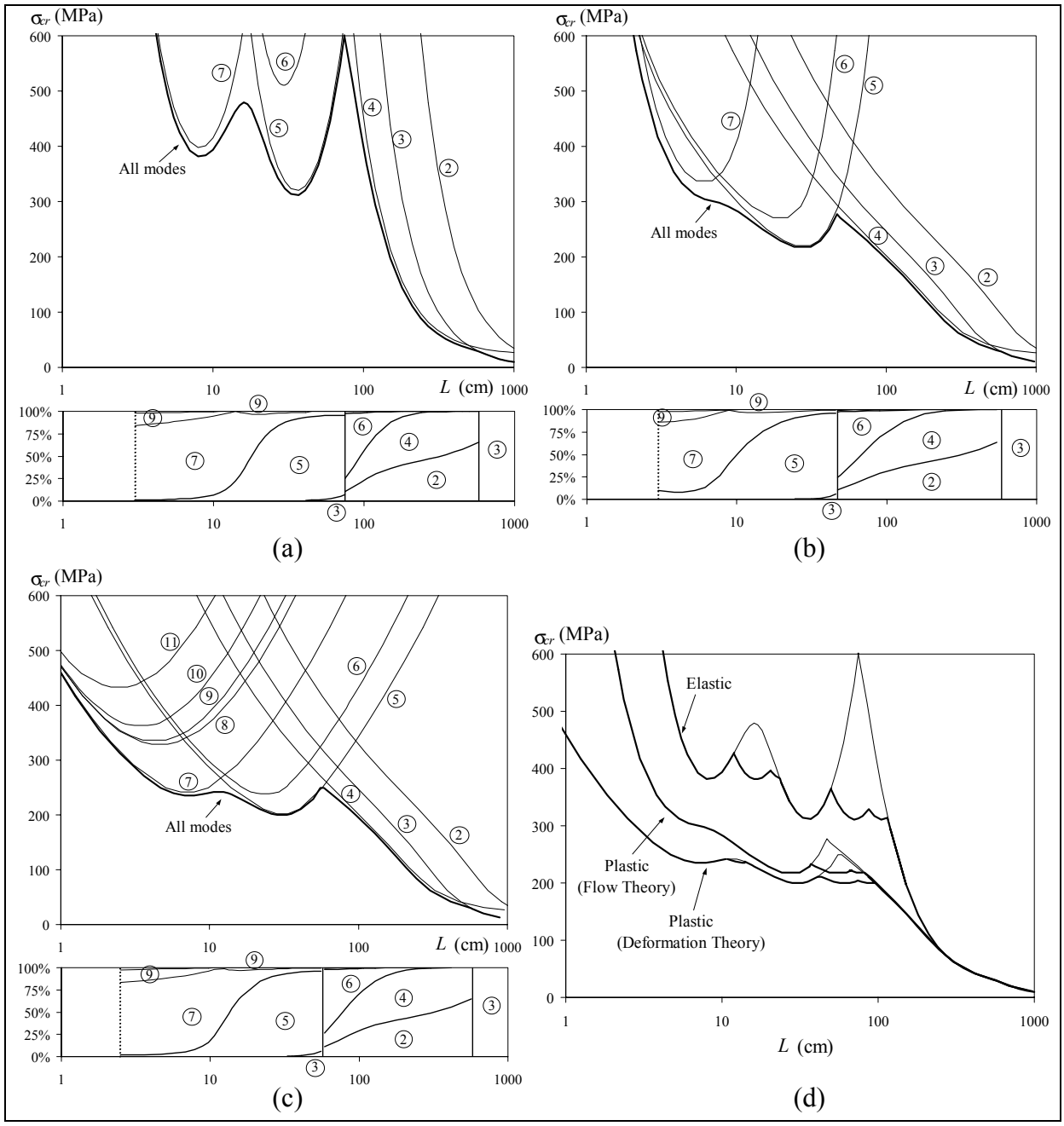

Figure 6 C-section column results: (a) linear elastic (m=1), (b) elastic-plastic (flow) (m=1), (c) elastic-plastic (deformation) (m=1) and (d) "true" critical stresses (m≥1)

3.3 Illustrative example: rectangular hollow section columns

Finally, the buckling behaviour of rectangular hollow section (RHS) columns is addressed. As before, (i) all the columns analysed are simply supported and have free-to-warp end sections and (ii) the material properties read E_0=200GPa, ν=0.3, $\sigma_{0.2}$=300MPa, n=5. The cross-section dimensions are given in Figure 7 and the GBT discretisation now involves 4 natural and 10 intermediate nodes (3 per web and 2 per flange), which means that 15 deformation modes are obtained: extension ①, minor ② & major ③ axis bending, torsion ④, distortion ⑤ and 10 local-plate modes. Figure 7 displays the shapes of the first 10 modes.

A preliminary exact GBT analysis showed that modes ④ and ⑤ do not participate in the column critical buckling mode, which is due to the very high torsional stiffness of closed thin-walled sections (particularly when compared with the stiffness of open sections). Thus, these two modes were disregarded, a decision which led again to some computational savings without affecting the accuracy of the results. All the remaining 13 modes were included in the buckling analyses.

Once more, the curves presented in Figures 8(a) (linear elastic), 8(b) (flow theory) and 8(c) (deformation theory) show the variation of σ_{cr} with L, for m=1. The thin lines correspond again to buckling in individual GBT modes and the thick ones to buckling in the combination of the GBT modes leading to the lowest σ_{cr} (mixed buckling mode). The mode participation factor diagrams are displayed in the bottom part of Figures 8(a)–(c) and Figure 8(d) shows "all mode" curves (i) concerning the three material behaviours and (ii) associated to m=1 (thin lines) and m≥1 (thick lines).

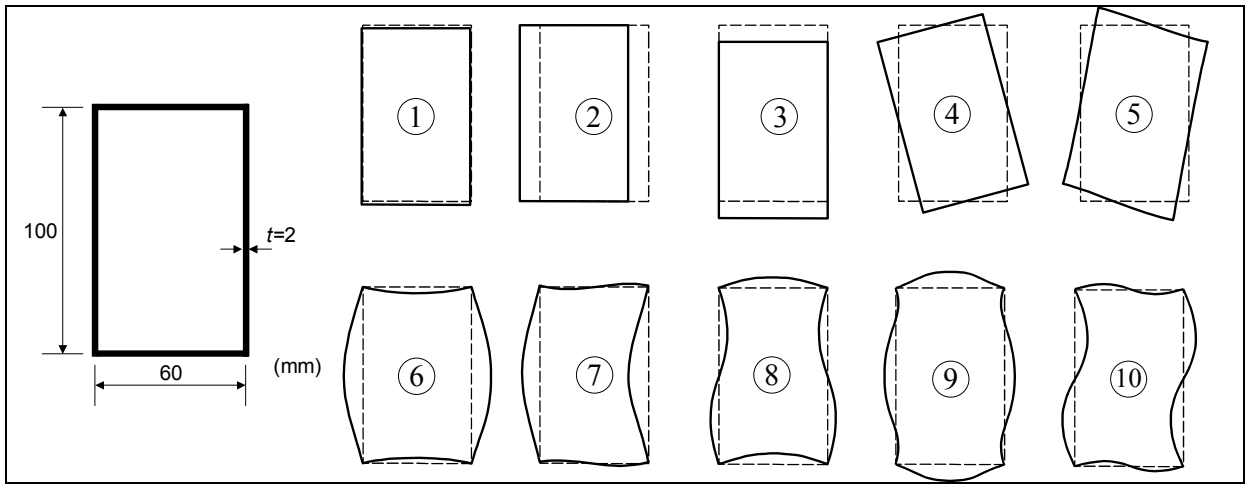

Figure 7 RHS cross-section geometry and first ten GBT deformation mode shapes

Since the existing validation of the GBT for the bifurcation analysis of (linear elastic) closed section (tubular) thin-walled members [16] is not yet available (published), Figure 8(d) includes also results obtained from FEM analyses performed by means of the commercial code ABAQUS [24] and using four node shell (S4) finite elements to discretise the columns. These results consist of (i) a curve providing the variation of the "true" critical stresses (m≥1) with the column length L and (ii) three critical buckling mode configurations (displayed on the top part of Figure 8(d)). One immediately observes that the (i) (linear elastic) GBT and (ii) FEM curves practically coincide (differences below 1%), which provides evidence to validate the proposed linear elastic GBT formulation for tubular members [16].

The observation of the curves shown in Figures 8(a)–(d), as well as the comparison with the corresponding ones presented in Figures 6(a)–(d) (note that the vertical scales are the same in both sets of figures), leads to the following conclusions:

(i) The major difference between the buckling behaviour of C-section and RHS columns stems from the relevant role played by the torsion and distortional modes in the former case (modes ④, ⑤ and ⑥ in Figure 5). Since they are absent in RHS columns, the critical buckling modes basically involve flexural (global) and local-plate modes. Indeed, Figures 8(a)–(c) show, for m=1, the following mode participation: (a) short to intermediate columns buckle in the web-triggered symmetric local-plate mode ⑥, (b) a mixed anti-symmetric local-plate-flexural mode (⑦+②) occurs for intermediate columns and, as expected, (c) long columns buckle in the "pure" weak-axis flexural mode ②.

(ii) As for the C-section columns, one has that (a) the elastic-plastic bifurcation stress values are lower than the elastic ones (except for long columns – $\Lambda_T \approx \Lambda_S \approx 1$), (b) J_2 deformation theory leads to lowest values, (c) the curves concerning the individual flexural modes ② and ③ have been shown to reproduce the results yielded by the tangent modulus formulae and (d) the transition between local-plate and global critical modes is less "abrupt" in either of the elastic-plastic cases.

(iii) It is interesting to notice the presence of a much larger number of "individual mode" curves in Figures 6(c) & 8(c), when compared with the ones appearing in Figures 6(a) & 8(a) and 6(b) & 8(b). This is due to the fact that J_2 deformation theory predicts a very pronounced erosion of the $\dot{E}_{ij}$ values, which significantly lowers several higher-order "local-plate" curves, thus making them visible in the figure.

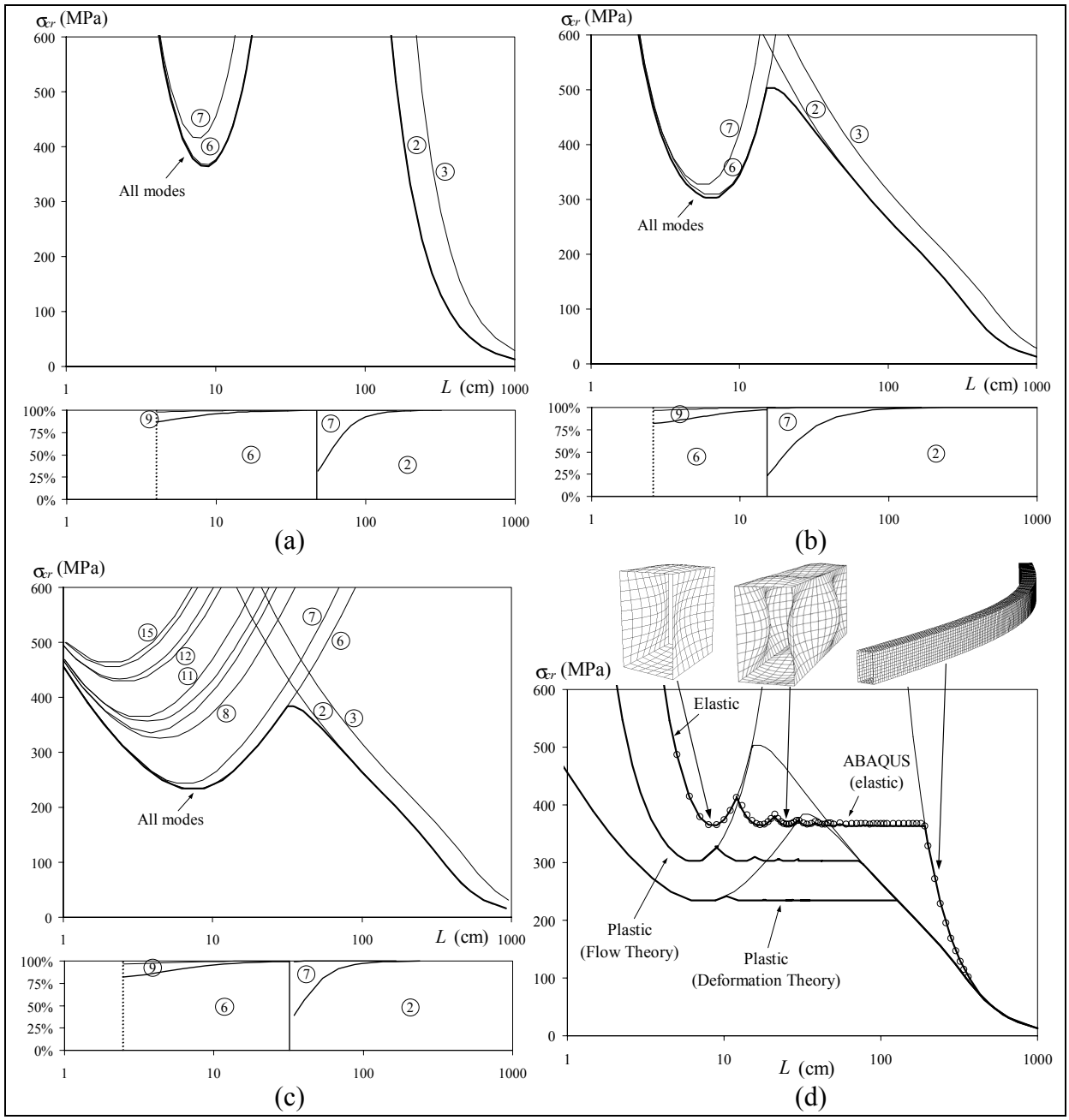

Figure 8 RHS column results: (a) linear elastic (m=1), (b) elastic-plastic (flow) (m=1), (c) elastic-plastic (deformation) (m=1) and (d) "true" critical stresses ($m \geq 1$)

4 CONCLUSION

The formulation of a non-linear elastic Generalised Beam Theory (GBT), enabling the assessment of the local and global buckling behaviour of open and closed thin-walled columns (uniformly compressed members), was briefly overviewed and particular attention was paid to (i) the specific procedures required to handle the material non-linearity and to (ii) the evaluation of the adequate instantaneous elastic moduli. The proposed formulation was then validated, by means of its application to a plate buckling problem for which analytical solutions have been reported in the literature. Finally, GBT stability analyses were performed to investigate the local-plate, distortional and global buckling behaviour or C-section and RHS stainless steel columns. The material behaviour was modelled using a Ramberg-Osgood stress-strain law and the relevant instantaneous elastic moduli were evaluated on the basis of both J_2 flow and deformation plasticity theories.

Future work includes (i) assessing the differences in column buckling behaviour stemming from using the "improved" Ramberg-Osgood stress-strain law recently proposed by Mirambell & Real [22], (ii) determining the buckling behaviour of stainless steel columns with other (commonly used) cross-section geometries (shape and dimensions), (iii) extending the GBT formulation to additional applied stress distributions (*e.g.*, combinations of uniform compression and pure bending), thus enabling the analysis of beams and beam-columns, and, finally, (iv) exploring the unique features and capabilities of the GBT analyses, namely for the development of efficient design formulae and/or procedures for stainless steel thin-walled members.

5 REFERENCES

[1] Nethercot, D. & Gardner, L. (2002). "Exploiting the Special Features of Stainless Steel in Structural Design", *Advances in Steel Structures* (9-11 December Hong Kong Conference Proceedings), S.L. Chan, J.C. Teng & K.F. Chung (eds.), vol. 1, Elsevier, Amsterdam, 43-55.

[2] Galambos, T.V. (ed.) (1998). *Guide to Stability Design Criteria for Metal Structures*, John Wiley & Sons, New York.

[3] Gardner, L., Nethercot, D. & Estrada, I. (2002). "An Efficient Method for Designing Stainless Steel Structures", *Proceedings of the 2003 SSRC Annual Technical Session & Meeting*, April 2-5, SSRC, Baltimore, 473-492.

[4] Comité Européen de Normalisation (CEN) (1996). *Eurocode 3: Design of Steel Structures, Part 1-4: General Rules – Supplementary Rules for Stainless Steel (ENV 1993-1-4)*, Brussels.

[5] Shanley, F.R. (1947)."Inelastic Column Theory", *Journal of the Aeronautical Sciences*, **14**, 261-268.

[6] Hill, R. (1958). "A General Theory of Uniqueness and Stability in Elastic-Plastic Solids", *Journal of Mechanics and Physics of Solids*, **6**, 236-249.

[7] Hutchinson, J.W. (1974). "Plastic Buckling", *Advances in Applied Mechanics*, **14** (ed. C.-S. Yih), Academic Press, New York, 67-144.

[8] Tvergaard, V. & Needleman, A. (1982). "On the Foundations of Plastic Buckling", *Developments in Thin-Walled Structures – 1*, J. Rhodes & A.C. Walker (eds.), Elsevier Applied Science, 205-233.

[9] Rasmussen, K.J.R., Burns, T., Bezkorovainy, P. & Bambach, M.R. (2002). "Numerical Modelling of Stainless Steel Plates", *Advances in Steel Structures* (9-11 December Hong Kong Conference Proceedings), S.L. Chan, J.C. Teng & K.F. Chung (eds.), vol. 2, Elsevier, Amsterdam, 617-624.

[10] Schardt, R. (1989). *Verallgemeinerte Technishe Biegetheorie*, Springer-Verlag, Berlin.(in german)

[11] Leach, P. & Davies, J.M. (1996). "An Experimental Verification of the Generalised Beam Theory Applied to Interactive Buckling Problems", *Thin-Walled Structures*, **25**(1), 61-79.

[12] Davies, J.M. (1999). "Modelling, Analysis and Design of Thin-Walled Steel Structures", *Light-Weight Steel and Aluminium Structures* (June 20-23 Helsinki Conference Proceedings), P. Mäkeläinen & P. Hassinen (eds.), Elsevier, Amsterdam, 3-18.

[13] Silvestre, N. & Camotim, D. (2002). "First Order Generalised Beam Theory for Arbitrary Orthotropic Materials, *Thin Walled Structures*, **40**(9), 755-789.

[14] Silvestre, N. & Camotim, D. (2002). "Second Order Generalised Beam Theory for Arbitrary Orthotropic Materials, *Thin Walled Structures*, **40**(9), 791-820.

[15] Gonçalves, R. & Camotim, D. (2003). "Buckling Behaviour of Thin-Walled Aluminium and Stainless Steel Columns Using Generalised Beam Theory", *Advances in Structures* (ASSCCA'03 – June 23-25 Sydney Conference Proceedings), G. Hancock, M. Bradford, T. Wilkinson, B. Uy & K. Rasmussen (eds.), Balkema Publishers, Lisse, 405-411 (vol.1).

[16] Gonçalves, R., Camotim, D. & Dinis, P.B. (in preparation). "Generalised Beam Theory to Analyse the Buckling Behaviour of Closed-Section Elastic and Elastic-Plastic Thin-Walled Members".

[17] Ramberg, W. & Osgood, W.R. (1943). "Description of Stress-strain Curves by Three Parameters", *NACA Tecnical Note nº 902*.

[18] Hill, H.N. (1944). “Determination of Stress-Strain Relations from the Offset Yield Strength Values”, *NACA Tecnical Note nº 927*.

[19] Chen, W.F. & Han, D. (1988). *Plasticity for Structural Engineers*, Springer-Verlag, New York.

[20] Handelman, G.H. & Prager, W. (1948). “Plastic Buckling of a Rectangular Plate Under Edge Thrusts”, *NACA Tecnical Note nº 1530*.

[21] Bijlaard, P. (1949). “Theory and Tests on the Plastic Stability of Plates and Shells”, *Journal of the Aeronautical Sciences*, **16**, 529-541.

[22] Mirambell, E. & Real, E. (2000). “On the Calculation of Deflections in Structural Stainless Steel Beams: an Experimental and Numerical Investigation”, *Journal of Constructional Steel Research*, **54**(1), 109-133.

[23] Silvestre, N., Simão, P., Camotim, D. & Silva, L. (2001). “Application of Generalised Beam Theory (GBT) to the Stability Analysis of Cold-Formed Steel Members”, *Proceedings of the Third National Conference on Steel and Composite Construction*, A. Lamas, P. Vila Real & L. Silva (eds.), Aveiro (December 6-7), 617-626. (in portuguese)

[24] Hibbit, Karlsson & Sorensen Inc. (2002) *ABAQUS Standard* (Version 6.3-1).